A FLEXURE-BASED MULTI-LAYER ROLL-TO-ROLL PRINTING SYSTEM

Chenglin Li and Shih-Chi Chen*
Department of Mechanical and Automation Engineering
The Chinese University of Hong Kong
Shatin, N.T., Hong Kong SAR, China
*Email: scchen@mae.cuhk.edu.hk

In this paper, we present the design and characterization of a fully automated flexure-based multi-layer roll-to-roll (R2R) printing system for continuous fabrication of multi-layer devices. The new R2R system achieves nanometer level multi-axis positioning precision and submicron level cross-layer registration precision via the development of a five-axis roller positioner and a new vision-based alignment method that enables the use of two low resolution cameras to achieve nanometer level precision.

PRECISION MULTI-LAYER R2R PRINTING

R2R printing technologies, e.g., gravure and flexography, have been widely utilized in many emerging applications such as organic photovoltaic (OPV) devices and flexible electronics. They present tremendous advantages in terms of cost and throughput. Recently, contact printing techniques, e.g., MCP and nanoimprint lithography (NIL), have been successfully implemented on R2R platforms, driving the print resolution of R2R platforms to submicron level [1, 2]. However, one critical issue to be addressed in the aforementioned R2R systems is that they lack the capability to register the patterns precisely across layers, which fundamentally limits the system to produce complex and functional devices. Although new multi-axis precision alignment methods, e.g., vision-based method (~200 nm/ sub-microradian for linear/angular alignment) [3], have been proposed and demonstrated, they have never been applied to state-of-the-art R2R systems to realize multi-layer printing.

To realize multi-layer precision R2R printing, one must have a (1) multi-axis positioner for controlling the rollers with nanometer level repeatability and precision, and (2) practical metrology solution that provides nanometer level accuracy for in-plane measurements. Current R2R systems use conventional bearings to guide the printing motion, resulting in low repeatability and precision; these R2R systems also lack the required degrees of freedom (DOF) to correct the "roll" and "yaw" errors of the roller, i.e., rotational errors in the θ_X and θ_Y directions respectively as illustrated in Fig. 1, resulting in non-uniform distribution of the print pressure (Fig. 1A) and angular misalignment between the patterned layers (Fig. 1B). To address these issues, we will use flexures [4-7] to design precise and highly repeatable mechanisms to guide the motion of rollers in a R2R system.

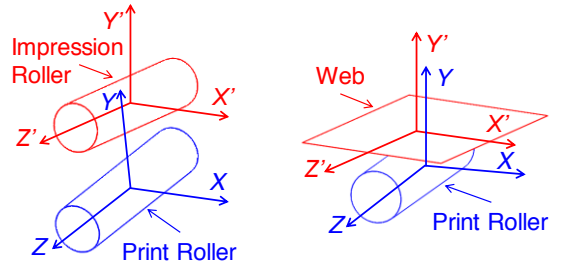

A B

FIGURE 1. Illustration of different types of misalignments in a R2R system. A: "roll" error; B: "yaw" error.

FIVE-AXIS ROLLER POSITIONER

Previously, we have developed a flexure-based R2R system for single-layer large-area continuous printing [1, 8-9], achieving a 100 nm print resolution on a 4" web. Based on this work, we have developed a five-axis roller positioner to realize precision multi-layer R2R printing for fabricating complex devices of 100s nm resolution. The challenge lies in the precise position control between the web and the print roller, to which the stamp is attached.

Figure 2 presents the CAD model of the five-axis roller positioner, where two monolithic compliant *X*-*Y* stages are installed to support and guide the compliant *Z* stage. The print roller is mounted on the *Z*-stage so that it has five DOF error correction capability, i.e., *x*, *y*, *z*, θ_X, and θ_Y. Each *X*-*Y* stage is driven by two voice coil actuators (VCA) (X_I, X_O, Y_I, and Y_O, NCC03-15-

050-2X, H2W) and provides decoupled motion guidance capability in the *X* and *Y* axes. The compliant *Z* stage is also driven by a VCA (*Z*, NCC05-18-060-2PBS, H2W). VCAs are used due to their high bandwidth (400 Hz) and high force output (~28 N/Amp). A stepper motor (NEMA 23, NI) is connected to the shaft, i.e., print roller, with an elastomeric coupler and controls the printing process (motion in θ_Z).

Figure 3 presents simulated results of the five-axis positioner, which yields decoupled motions in five axes, i.e., *x*, *y*, *z*, θ_X, and θ_Y.

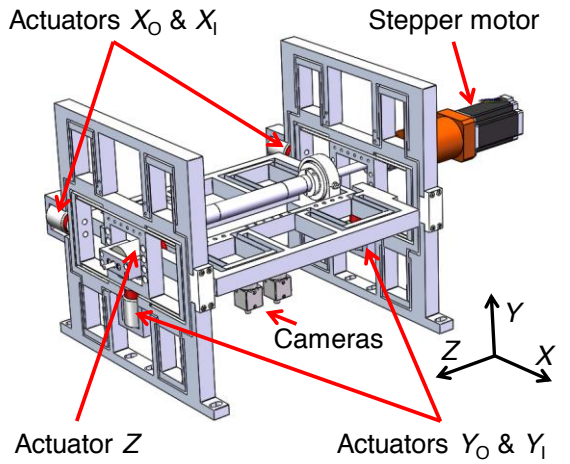

FIGURE 2. CAD model of the flexure-based five-axis roller positioner

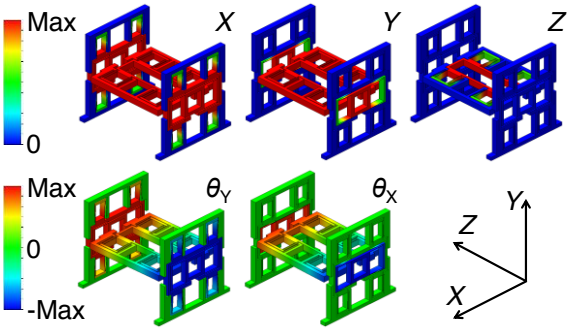

FIGURE 3. Simulated results of the five-axis positioner, demonstrating decoupled motion control in the X, Y, Z, θ_X, and θ_Y axes.

ASSEMBLY AND CHARACTERIZATION

To characterize the dynamic properties of the five-axis roller positioner, an impulse response experiment is conducted. Based on the measured displacement data from the capacitance probes, resonant frequencies in different axes are calculated by fast Fourier transform (FFT). Table 1 summarizes the performance specifications of the positioner, including the resonant frequencies, strokes, and minimum increments in all six axes.

TABLE 1. Specifications of the five-axis roller positioner.

	Frequencies	Strokes	Min. increments
X	10.0 Hz	±1 mm	50 nm
Y	9.5 Hz	±1 mm	75 nm
Z	19.0 Hz	±1 mm	200 nm
θ_X	32.5 Hz	±1 mrad	2 μrad
θ_Y	28.0 Hz	±1 mrad	2 μrad
θ_Z	83.5 Hz	-	-

To characterize the cross-axis motion coupling effect, static displacement experiments are performed to identify the matrix, S_X, that maps actuator input voltages, X_A, to mechanism displacements, X_C. Six capacitance probes are fixed on a vibration isolation table to monitor the motions of the roller positioner. Assuming small displacements, Eqs. (1) and (2) can be used to obtain the matrix S_X [10]. The analytical solution of S_X is shown in Eq. (3), where a, b, c, d, and e are constant parameters related to the characteristics of the VCAs and flexural stages. The analytical S_X indicates that the motions in the *X*, *Y*, and *Z* axes are decoupled. Nevertheless, due to manufacturing errors and misaligned actuators and sensors, the measured S_X has deviations, and the motions in different axes are coupled to a certain degree. The measured results are shown in Eq. (4). The units used in Eqs. (1)–(4) are microns, microradians and millivolts.

$$X_C = S_X X_A \rightarrow \left[\Delta x \quad \Delta\theta_y \quad \Delta y \quad \Delta\theta_x \quad \Delta z\right]^{\mathrm{T}} = S_X \left[x_{\mathrm{I}} \quad x_{\mathrm{O}} \quad y_{\mathrm{I}} \quad y_{\mathrm{O}} \quad z\right]^{\mathrm{T}} \tag{1}$$

$$X_A = S_X^{-1} X_C \tag{2}$$

$$S_X = \begin{bmatrix} a & a & 0 & 0 & 0 \\ b & -b & 0 & 0 & 0 \\ 0 & 0 & c & c & 0 \\ 0 & 0 & -d & d & 0 \\ 0 & 0 & 0 & 0 & -e \end{bmatrix} \tag{3}$$

$$S_X = \begin{bmatrix} 2.35 & 2.45 & 0.15 & -0.13 & -0.07 \\ 2.93 & -2.86 & -0.07 & 0.05 & 0.07 \\ -0.07 & 0.23 & 2.12 & 1.04 & -0.04 \\ 0.02 & -0.04 & -2.57 & 3.43 & -0.09 \\ -0.55 & 0.58 & 0.04 & 0.02 & -1.46 \end{bmatrix} \tag{4}$$

POSITIONING EXPERIMENTS

Static positioning experiments in selected axes (*X*, *Z*, and θ_Y) are performed to demonstrate the precision of the roller positioner. In these experiments, the matrix, S_X^{-1} , is used in a closed-loop PID controller for correction, and the position feedback signals are obtained from the six capacitance probes. Figure 4 plots the measured displacements (left column) and off-axis errors (right column) versus closed-loop displacement commands. The results show that the off-axis translational and rotational errors are controlled within ±50 nm in *X*/*Y*/*Z* axes, and ±100 nrad in θ_X/θ_Y axes; the errors are comparable to the resolution of the capacitance probes (C8/CPL190, Lion Precision, resolution: 20 nm).

Figure 5 presents the positioning results in all five axes under the PID control. In this experiment, the positioner is commanded to perform 10-*μ*m and 30-*μ*rad steps in the *X*, *Y*, *Z*, θ_X and θ_Y axis in a sequential fashion, with each step held for 20 seconds. As Fig. 5 shows, the motion in one axis does not affect motions in other five axes. It is found that, under closed-loop control, the *X*, *Y*, *Z*, θ_X and θ_Y axes have a resolution of ±100 nm, ±200 nm, ±200 nm, ±2 *μ*rad and ±2 *μ*rad respectively. Note that error motions in θ_Z axis are mainly caused by manufacturing errors, which are relatively small, i.e., within ±3 *μ*rad in this experiment.

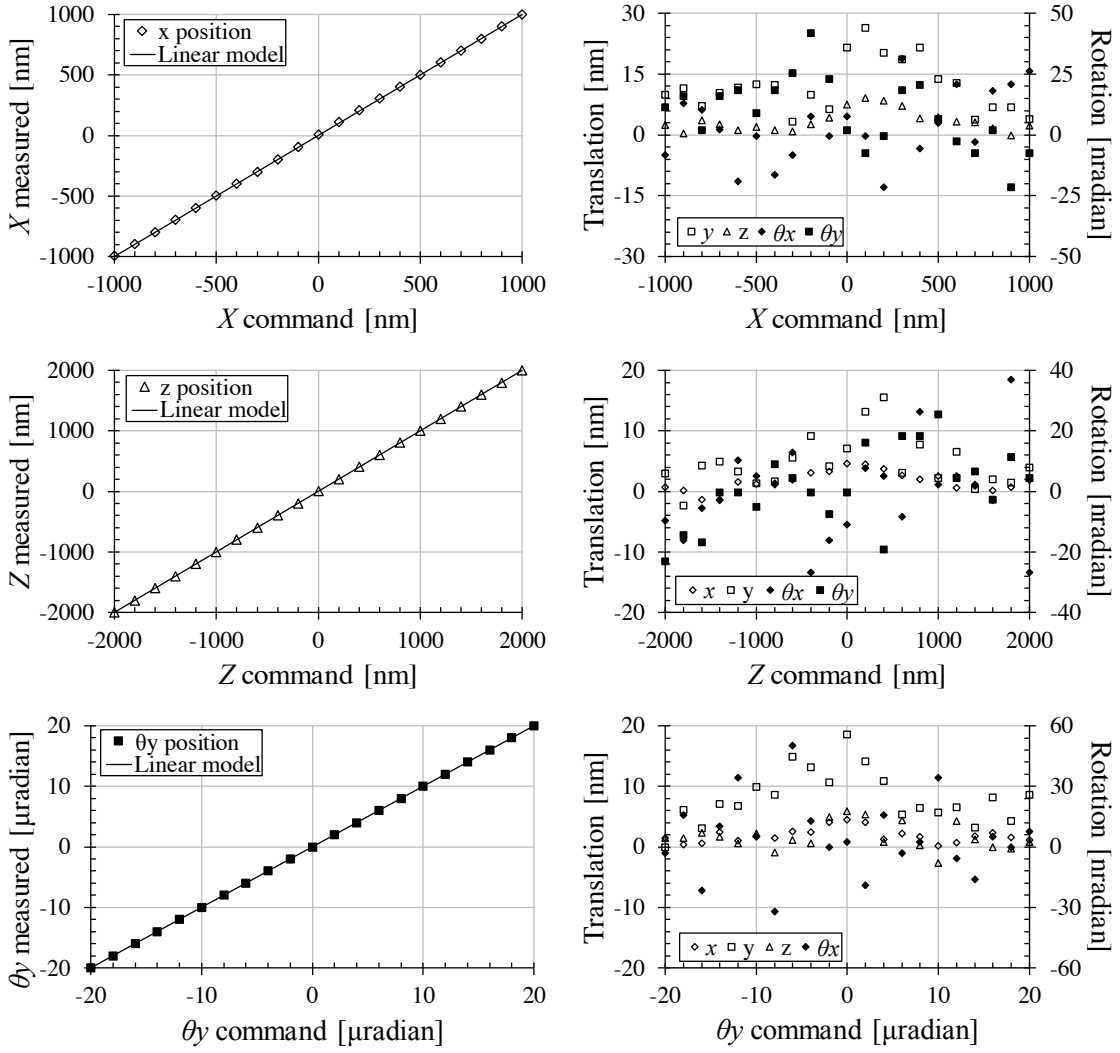

FIGURE 4. X, Z, and θ_Y positioning results under closed-loop control.

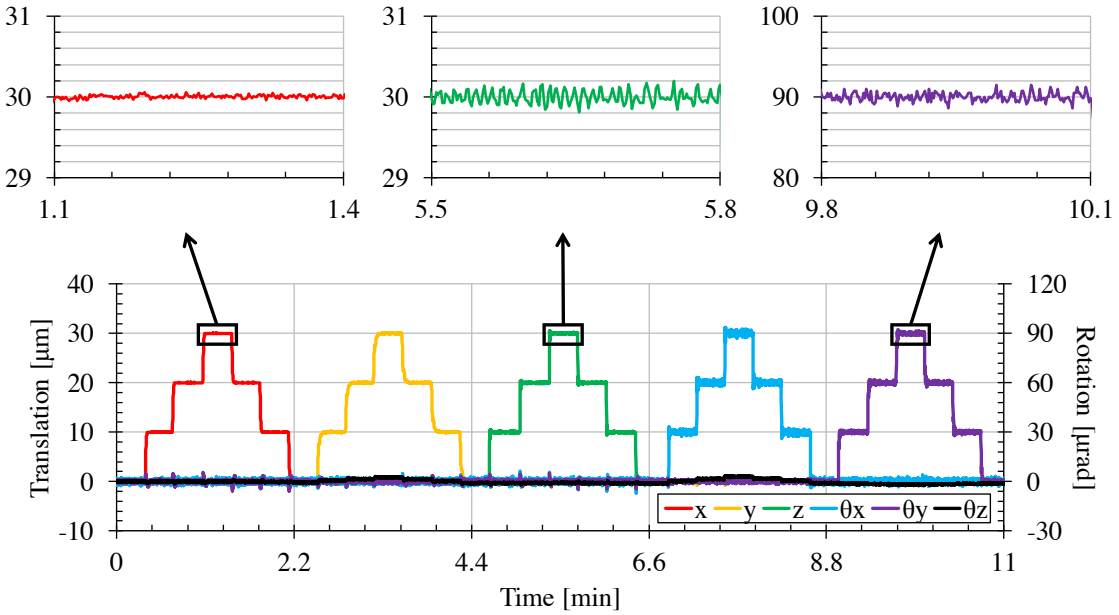

FIGURE 5. Positioning results in all five axes, i.e., X, Y, Z, θ_X, and θ_Y axes, with PID control

MULTI-LAYER ALIGNMENT – SIMULATION AND VERIFICATION

In this section, we present a vision-based method that employs two low resolution cameras to achieve nanometer level precision. Inspired by the vision-based absolute planar encoder design [3, 11], we have designed a new hybrid alignment mark, as shown in Fig. 6A, to be printed on the edges of the web along with the first layer patterns. The alignment mark consists of periodic grid patterns and cross marks. First, by comparing the position of the cross mark with the center of the camera, position measurement can be achieved with a resolution equal to the pitch of the grid pattern, i.e., 10s μm. Following that, a discrete Fourier transform (DFT)-based phase estimation method is used to determine the position within each period of the grid pattern, achieving nanometer level linear position measurement as well as sub-microradian level angular position measurement.

Simulated experiments are performed in MATLAB to verify the capability and feasibility of the alignment algorithm, where translational and rotational displacements are introduced to the image. In the experiment, the test alignment mark (Fig. 6C) has a resolution of 512 × 512 pixels, and the pitch of the 2D grid pattern is 4 pixels in both *X* and *Z* directions. Through pattern recognition of the cross mark, we can estimate the absolute position in the *X* and *Z* axes with a resolution of one pixel (~5 microns).

Next, the amplitude and phase spectrum of the image is obtained by 2D DFT (Fig. 6D and 6E). Based on the four fundamental frequency components (maximum amplitudes, red and green points in Fig. 6D), the absolute angular resolution is found to be ±4 milliradians. By analyzing the phase spectrum with the four fundamental frequency components, high resolution positioning sensing can be achieved, i.e., 0.3% error (~10s nm for practical application) in *X*/*Z* axes and ±0.5 microradians in θ_Y axis. Note that the angular position variation between successive images need to be less than 1 mrad in order to obtain the precision stated above.

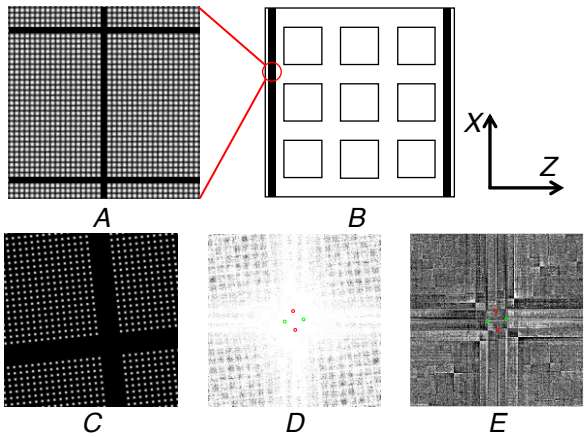

FIGURE 6. Design of the hybrid alignment mark (A) to be printed on the two edges of the web (B); MATLAB simulation results: hybrid alignment mark with displacements in X/Z/θ_Y

axes (C), and its spectrum in amplitude (D) and phase (E). The red and green points show the fundamental frequency components.

SYSTEM INTEGRATION

Figure 7 presents the prototype multi-layer R2R printing system, integrated with the five-axis roller positioner. The system includes a rewinding module, unwinding module, tension control module, web guide module, and two printing modules, where the right one prints the first layer, and the left one registers and prints the subsequent layers.

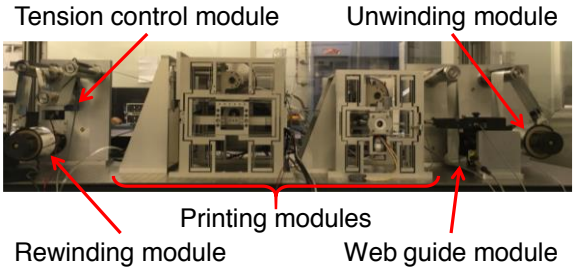

FIGURE 7. Prototype flexure-based R2R system with integrated five-axis roller positioner for precision multi-layer printing

CONCLUSION

We have presented the design and characterization of a flexure-guided five-axis roller positioner and a new vision-based alignment method for multi-layer R2R printing, achieving 100s nanometer positioning and registration precision. The roller positioner is driven by five high performance VCAs, where capacitance probes are used to monitor the displacement in different axes in real time. Closed-loop control is implemented to the system, achieving a resolution ±50 nm in *X*/*Y*/*Z* axes, and ±100 nrad in θ_X/θ_Y axes. These promising results show that R2R fabrication may achieve comparable resolution with photo-lithography at a much lower cost.

ACKNOWLEDGMENT

This work is supported by the HKSAR Research Grants Council (RGC), Theme Based Research Scheme (TRS), T23- 407- 13N.

REFERENCES

[1] Zhou X, Wang D, Wang J, and Chen S. Precision Design and Control of a Flexure-based Roll-to-roll Printing System. Precision Engineering. 2016, 45, 332-341.

[2] Ahn SH, Guo LJ. Large-area Roll-to-roll and Roll-to-plate Nanoimprint Lithography: A Step toward High-throughput Application of Continuous Nanoimprinting. ACS Nano. 2009, 3(8), 2304-2310.

[3] Cao Z, Chen Z, and Huang PS. A Vision-based Absolute Planar Encoder for High Precision In-plane Position Measurement. Proc. of the Annual Meeting of the ASPE, Portland, OR, USA, Oct. 2016, pp.161-66.

[4] Howell L. Compliant Mechanisms. John Wiley and Sons Inc. New York: 2001.

[5] Li C, Wang J, and Chen S. "Flexure-based Dynamic-tunable Five-axis Nanopositioner for Parallel Nanomanufacturing. Precision Engineering. 2016, 45, 423-434.

[6] Chen W, Yang S, Liu J, Chen W, and Jin Y. Design of a Novel 5-DOF Flexure-based Compound Alignment Stage for Roll-to-roll Printed Electronics. Review of Scientific Instruments. 2017, 88(2), 025002.

[7] Paolo B. Design and Development of High Precision Five-axis Positioning System for Roll-to-roll Multi-layer Microcontact Printing. Master Thesis. Massachusetts Institute of Technology. 2009.

[8] Zhou X, Xu H, Cheng J, Zhao N, and Chen S. Flexure-based Roll-to-roll Platform: A Practical Solution for Realizing Large-area Microcontact Printing. Scientific Reports. 2015, 5, 10402.

[9] Wang D, Zhou X, and Chen S. Control Strategy for Flexure-based Precision Roll-to-roll Machine. Proc. of the Annual Meeting of the ASPE, Austin, TX, USA, Nov. 2015, pp.27-31.

[10] Culpepper ML, Anderson G. Design of a Low-cost Nano-manipulator which Utilizes a Monolithic, Spatial Compliant Mechanism. Precision Engineering. 2004, 28(4), 469–482.

[11] Chen ZH, and Huang PS. A Vision-based Method for Planar Position Measurement. Measurement Science and Technology. 2016, 27(12), 125018.